Tubular aryl hydrocarbon receptor upregulates EZH2 to promote cell senescence in cisplatin-induced acute kidney injury

Li Wen
Division of Nephrology, West China Hospital of SCU
Qian Ren
West China Hospital of Sichuan University
Xiaoyan Du
West China Hospital
Hongliu Yang
Division of Nephrology, West China Hospital of SCU
Fan Guo
Division of Nephrology, West China Hospital of SCU https://orcid.org/0000-0002-7329-5124
Liang Ma (liang_m@scu.edu.cn)
West China Hospital of Sichuan University https://orcid.org/0000-0001-8327-7969
Ping Fu
Division of Nephrology, West China Hospital of SCU https://orcid.org/0000-0002-3061-5925

Article

Keywords: Acute kidney injury, aryl hydrocarbon receptor, enhancer of zeste homolog 2, cellular senescence

Posted Date: August 1st, 2022

DOI: https://doi.org/10.21203/rs.3.rs-1848869/v1

Version of Record: A version of this preprint was published at Cell Death & Disease on January 12th, 2023. See the published version at https://doi.org/10.1038/s41419-022-05492-3.

Abstract

Acute kidney injury (AKI) is one of the serious clinical syndromes with high morbidity and mortality. Despite substantial progress in understanding of AKI mechanism, no drug therapy is available for treatment or prevention. In this study, we identified that a ligand-activated transcription factor aryl hydrocarbon receptor (AhR) was highly expressed in the kidneys of cisplatin-induced AKI mice or tubular epithelial TCMK-1 cells. Notably, the AhR inhibition by BAY2416964 and tubular conditional deletion both alleviated cisplatin-induced kidney injury and cellular senescence, which was indicated by senescence-associated β-galactosidase (SA-β-gal) activity, biomarker p53, p21, p16 protein expression, and secretory phenotype IL-1β, IL-6 and TNFα level. Mechanistically, the abnormal AhR expression was positively correlated with the elevated EZH2, a methyltransferase. In addition, AhR inhibition also could suppress the EZH2 expression in the cisplatin-injured kidneys. Furthermore, the ChIP assay displayed that EZH2 may indirectly interact with AhR promoter region by affecting H3K27me3. The direct recruitment between H3K27me3 and AhR promoter is higher in the kidneys of control than that of cisplatin mice, suggesting EZH2 could reversely regulate the AhR expression through weakening H3K27me3 transcriptional inhibition on AhR promoter. Collectively, the present study implicated that AhR and EZH2 have mutual regulation, which further accelerated tubular cellular senescence in cisplatin-induced AKI.

Introduction

Acute kidney injury (AKI) is a common clinical syndrome and a major health issue, which refers to a rapid decline of kidney function in a short period of time caused by a variety of factors, such as renal hypoperfusion, trauma, sepsis, and toxic drugs, etc (1–3). Approximately 13.3 million people suffer from AKI every year (4), and 30%~70% of AKI patients develops into chronic kidney disease (CKD) or end-stage kidney disease (ESKD) (5), and about 1.7 million of the deaths are caused by AKI (6, 7). As we known, cisplatin is an antitumor chemotherapy drug, but one-third of cancer patients receiving cisplatin chemotherapy are susceptible to AKI (8). However, practical strategies for treating cisplatin-induced AKI still seem to be lacking. Therefore, focusing on the mechanism of cisplatin-induced AKI is of great significance for drug discovery and the improvement in the quality of the population associated with cisplatin nephrotoxicity.

The increasing studies have shown that cisplatin could stimulate oxidative stress and induce cellular senescence (9), which may even promote AKI to CKD transformation (10). Notably, oxidative stress has emerged as a major cause of cellular senescence (9) and oxidative stress-mediated cellular senescence has been found to induce cisplatin-induced interstitial fibrosis (11, 12). In cisplatin-induced cultured tubular cells, mitochondrial dysfunction, accompanied by excessive reactive oxygen species (ROS) production, leads to severe damage (13). Mitochondrial dynamics improvement and cellular premature senescence repression contribute to exerting reno-protective effects (12, 14). To date, considerable studies have focused on cisplatin nephrotoxicity, whereas very little is known about molecular mechanism by which cisplatin caused cellular senescence in the injured kidneys.

Aryl hydrocarbon receptor (AhR) is a ligand-activated transcription factor, which can change conformational and expose the nuclear transfer site after binding to its ligand, along with binding to aromatic hydrocarbon receptor nuclear transfer proteins (ARNT) to regulate the expression of target genes (15, 16). Few efforts have play attention to AhR-related mechanisms of AKI until now. Our previous study showed that AhR activation triggers inflammation and apoptosis in rhabdomyolysis and ischemia-reperfusion (IR) induced AKI (17). Furthermore, AhR pathway activation contributes to tubular epithelial cellular senescence under anoxia or reoxygenation (18). Dramatic AhR upregulation in cisplatin-induced AKI points to AhR as a critical factor inducing oxidative stress. However, whether AhR upregulation participates in cellular senescence of cisplatin-induced AKI and its potential mechanisms need to be further explored.

Thus, in this study, we aimed to explore the possible mechanisms of AhR-mediated cellular senescence and identify AhR as a potential drug target against cisplatin-induced AKI. Here, the present results indicated that the inhibition of AhR alleviates cisplatin-induced oxidative stress and cellular senescence, further treats kidney injury, which may be closely related to the reduction of EZH2, caused by AhR inhibition.

Results

The high expression of renal tubular epithelial AhR aggravates cisplatin-induced AKI

The characteristics of AhR in kidneys by public data of single-cell sequencing were shown in Supplementary Fig. 1. Notably, there was an increase in the AhR expression across proximal tubule (PT) clusters after renal ischemia reperfusion injury at 4h (21). In this regard, we could propose that the expression of AhR in PT cells is up-regulated in IR-induced transient renal injury. Thus, based on the above single-cell data, we turn to consult the Gene Expression Omnibus database (No. GSE106993) and checked the RNA-sequencing data about cisplatin-stimulated mice (22). A clustered heatmap was shown in Fig. 1a, the RNA level of AhR was significantly upregulated in the kidneys of cisplatin-induced mice compared with that of control. Subsequently, we used immunofluorescence staining to detect the location and expression of AhR protein in cisplatin renal toxicity mice. In the kidneys of cisplatin mice, the fluorescence intensity of AhR was enhanced in the renal tubule nucleus, indicating the upregulation and activation of AhR in tubules (Fig. 1b). The expression of AhR by an antagonist BAY2416964 treatment was markedly reduced. Consistently, the mRNA and protein levels of AhR were increased after cisplatin stimulation, whereas both of them were substantially decreased by BAY2416964 treatment (Fig. 1c, d).

Importantly, the inhibition of AhR with BAY2416964 reduced the Scr, BUN levels, and kidney injury biomarker Kim-1, NGAL mRNA expression after cisplatin injection (Figure 1e). While the corresponding indicators remained unchanged when treated with BAY2416964 alone (Figure 1e). Meanwhile, the PAS staining displayed that AhR repression improved kidney pathological damages in the cisplatin-induced AKI mice, which was characterized by renal tubular dilation, loss of brush border, cast formation, and tubular epithelial cell apoptosis or necrosis (Figure 1f).

Consistent with the above results, the role of AhR was explored in tubular epithelial cell-specific deletion (tecKO) mice. The upregulation and activation of AhR were observed in WT cisplatin mice, but not in tecKO cisplatin mice (Figure 2a-c). Moreover, the kidney function as well as the mRNA and protein expression of Kim-1, NGAL were dramatically elevated in cisplatin-injected WT mice. As expected, conditional knockout of AhR played a positive renal protective effect, and the increase of corresponding indicators was not found in cisplatin-induced tecKO mice (Figure 2d-f, h). Importantly, conditional knockout of AhR could alleviate kidney pathological damages in cisplatin-induced AKI (Figure 2g). Taken together, these data indicated that the inhibition of AhR protected against cisplatin-induced kidney injury.

AhR promotes cellular senescence in cisplatin-induced AKI mice

Generally, the injured kidney could become a normal or near-normal kidney through the following tissue repair mechanisms, such as inflammatory infiltrate resolution, tubular proliferation, and epithelial repair or regeneration (23). However, maladaptive repair causes cell cycle arrest in the G2/M phase and releases senescence-associated secretory phenotypes (SASPs), which are the most critical risk factor of CKD progression after AKI (23). To explore whether AhR-induced kidney injury is related to cellular senescence, we detected the expression of senescence-associated β-galactosidase (SA β-gal) in the kidneys of cisplatin-induced AKI mice and the SA β-gal activity was significantly increased in the cisplatin-induced renal tubular cells, which was inhibited by AhR suppression with BAY2416964 (Figure 3a). Meanwhile, we also observed an obvious upregulation of senescence-associated genes (SAGs: p16, p21 and p53) and SASPs (IL-1β, IL-6, TNF-α) in the cisplatin mice by RT-qPCR and WB, and further BAY2416964 treatment repressed the expression of the corresponding SAGs and SASPs (Figure 3b-e). It has been reported that AhR activation in the heart generates excessive ROS(24), which may be responsible for cellular senescence (25). Thus, oxidative stress i was evaluated in the kidney of cisplatin-induced AKI mice. Consistent with previous results (26), xanthine oxidase (XO) level was increased, and anti-oxidant enzymes (Cat, Sod1, Sod2) levels were decreased in the cisplatin mice (Figure 3f). These results support a conclusion in which AhR activation induces oxidative stress by stimulating oxidase and repressing antioxidant enzymes. All above, AhR activation in cisplatin-induced AKI mice may show cellular senescence phenotype, which may be mediated by oxidative stress, whereas the specific mechanisms between them needs to be further explored.

Consistently, in cisplatin-induced AhR tecKO mice, lower SA β-gal expression was detected compared with WT mice (Figure 4a). Furthermore, the expression of SAGs (p16, p21 and p53) and SASPs (IL-1β, IL-6, TNF-α) were substantially inhibited in AhR specific deficiency cisplatin mice (Figure 4b-e). Similarly, the oxidase up-regulation and antioxidant enzymes down-regulation in WT cisplatin mice were observed, which were not present in AhR tecKO cisplatin mice. Combined with the above results are sufficient to confirm that AhR activation participates in regulating oxidative stress and cellular senescence in injured kidneys.

Knockdown of AhR alleviates cellular senescence and oxidative stress in cisplatin-stimulated TCMK-1 cells

Next, we carried out an AhR-siRNA transfection test to see if AhR knockdown could exert anti-cellular senescence and anti-oxidant stress effect *in vitro*. The best silencing efficacy AhR-siRNA#1 from the three transfection sequences was selected, and the mRNA and protein levels of AhR-siRNA#1 were markedly reduced (Figure 5a, b). After cisplatin stimulation, the mRNA levels of Kim-1 and NGAL were significantly up-regulated, while, AhR knockdown improved cisplatin-induced cell injury (Figure 5c). Consistent with the *in vivo* result, in cisplatin-induced TCMK-1 cells, the downregulation of AhR attenuated cisplatin-stimulated cellular senescence (Figure 5d, e), as evidenced by the reduction of SAGs (p16, p21 and p53) and SASPs (IL-6, TNF-α). In terms of oxidative stress, compared with negative control group, cisplatin stimulation up-regulated XO and down-regulated Sod1, Cat, while AhR knockdown reversed the expression of oxidative stress-related factors and suppressed oxidative stress response (Figure 5f-h).

AhR regulated EZH2 expression in cisplatin-injured kidneys and TCMK-1 cells

Previously, we have demonstrated that inhibition of EZH2 could reduce cisplatin-induced inflammation and improve renal injury (27). In pancreatic cancer cells, the activation of AhR/EZH2 signaling axis causes epigenetic alteration (28). Therefore, we explored the effect of AhR on the regulation of EZH2 in the kidneys of cisplatin-induced AKI mice. We made a correlation heatmap of our previous RNA-sequencing data and confirmed that the mRNA levels of AhR was highly related to EZH2 (Figure 6a). As expected, the expression of EZH2 and a transcription inhibition histone mark, H3K27me3 (Figure 6b, c), together with that of AhR (Figure 1b-d), were dramatically elevated in the kidneys of cisplatin-induced mice. Notably, both the transcription and translation levels of EZH2 were synchronously inhibited by AhR inhibition with BAY2416964 (Figure 6b, c), indicating that the expression of EZH2 is potentially regulated by AhR. Next, we used AhR tecKO mice to further verify the relationship between AhR and EZH2. Similarly, the upregulation of EZH2 and H3K27me3 were reversed by AhR deficiency after cisplatin stimulation (Figure 6d, e). In addition, as elaborated in Figure 5a, b and Figure 6f, g, AhR knockdown repressed the mRNA and protein expression of AhR and EZH2, simultaneously. Moreover, the expression of AhR and EZH2 were enhanced after cisplatin stimulation *in vitro*, whereas this upregulation was substantially reversed by AhR knockdown (Figure 6h, i). These results powerfully demonstrate that AhR upregulates the expression of EZH2, which may be positively correlated with the progression of tubular cell senescence in cisplatin-induced AKI mice.

AhR and EZH2 may exert physiological effects through reciprocally regulation

As found in the above experimental results, AhR regulates the expression of EZH2. However, as an essential epigenetic regulatory enzyme, EZH2 may play a transcriptional regulation role by affecting H3K27me3. Therefore, to explore whether EZH2 reversely regulates AhR, we further used EZH2 siRNA to detect the expression of AhR *in vitro*. The best silencing efficiency EZH2-siRNA#1 to transfect TCMK-1 cells was selected, and the mRNA and protein levels of EZH2 were dramatically reduced (Figure 7a, b). If AhR only regulates the expression of EZH2 unidirectionally, EZH2 knockdown does not affect AhR expression level. Actually, the expression of AhR was synchronously inhibited in TCMK-1 cells by EZH2 knockdown (Figure 7c, d), indicating that EZH2 silencing could repress the expression of AhR. Moreover,

the expression of EZH2 and AhR in cisplatin-treated TCMK-1 cells was found to be markedly higher than that in the untreated group, while their expression no longer rose by EZH2 silencing (Figure 7e-g). These data further highlight the potential effect that EZH2 regulates AhR expression, reversely.

Nevertheless, how does EZH2 affect the expression of AhR? Whether it has a relationship with the epigenetic effect of EZH2 or H3K27me3? In order to address this question, we used a ChIP assay to detect the enrichment between EZH2/H3K27me3 and AhR gene promoters *in vivo*. There are significant overlap peaks between AhR and EZH2 promoters in non-renal cells based on the ChIP-Atlas database. Hence, we designed AhR promoter primers on the basis of the overlapping peaks, and used the ChIP-qPCR assay to detect the enrichment between EZH2 and AhR gene promoters. No enrichment between EZH2 and AhR gene promoter regions was found (data not shown). Additionally, AhR-binding peaks significantly overlapped with H3K27me3 in renal cells on the genome level. ChIP-qPCR assay confirmed that H3K27me3 was bound to the AhR promoter regions in the control mice, while cisplatin stimulation reduced this enrichment (Figure 7h). These results indicate that the inhibition of H3K27me3 on AhR gene promoters was weakened, and the expression of AhR was up-regulated in cisplatin-induced AKI mice.

Discussion

Illustrating the potential mechanisms of AhR-induced cellular senescence is of great significance in identifying the cisplatin-induced AKI therapeutic targets. In this study, a novel finding, which was involved in AhR-associated cellular senescence leading to cisplatin-induced kidney injury, was remarkably proposed. We found that cisplatin induces cellular senescence both *in vivo* and *in vitro*, and the expression of AhR was positively associated with cellular senescence. Inhibition of AhR by BAY2416964 or tubule specific deletion of AhR significantly suppressed cellular senescence and alleviated cisplatin-induced renal injury. Notably, further studies indicated that EZH2, a histone methyltransferase, was a pivotal factor in AhR-induced cellular senescence in kidney injury.

Cellular senescence is a proven crucial process of AKI maladaptive repair or renal fibrosis (10). A previous study demonstrated that repeated low-dose cisplatin led to cell cycle arrest at the G2/M phase and cellular senescence, which mean cellular senescence played a vital role in cisplatin-induced kidney injury (29). Here, a cisplatin-induced AKI mouse model was generated using 20 mg/kg cisplatin. When the Scr value of the model group was higher than twice that of the control group, the cisplatin-induced AKI mouse model was considered successful. Moreover, an increase in β-galactosidase activity, a known characteristic of senescent cells, SAGs (p16, p21, p53) and SASPs (IL-1β, IL-6, TNF-α) were also observed in the cisplatin group compared with the control group. These results are consistent with those of Li et al., who confirmed that cisplatin induced cellular senescence in tubular epithelium, which could accelerate the progression of renal fibrosis (9).

AhR is an essential ligand-activated transcription factor (15). A distinct time-dependent and tissue-specific AhR activation is displayed in discrete mouse models of kidney disease (30). Growing evidence presented that AhR pathway activation by uremic toxins, like indoxyl sulfate, plays a significant harmful

role in CKD progression (31, 32). Whereas, the role of AhR in AKI remains controversial (17, 18). Tao et al. thought that AhR activation alleviated renal injury in rhabdomyolysis and I/R-induced AKI by inhibiting inflammation and apoptosis (17). Eleftheriadis et al. demonstrated that AhR pathway activation enhanced DNA damage response and promoted primary proximal renal tubular epithelial cells senescence, eventually leading to IR-induced kidney injury (18). Therefore, the contradictory effect of AhR was explored in our study. Here, our results revealed that AhR activation accelerated the progression of kidney injury through a cellular senescence-related mechanism in a cisplatin-induced AKI mouse model. Additionally, AhR inhibition by BAY2416964 or tubule specific deletion of AhR repressed cisplatin-induced cellular senescence, which implies that AhR may be one of the causative mechanisms of cisplatin-associated cellular senescence, and the inhibition of AhR to suppress cisplatin-induced cellular senescence may be a potential therapeutic strategy to attenuate kidney injury.

Although the relationship between AhR and tubular cellular senescence was observed in our study, we cannot clear the possible mechanisms of AhR-induced cellular senescence in cisplatin-induced AKI mice. EZH2, a catalytic subunit of polycomb repressive complex 2 (PRC2), is an H3K27 histone methyltransferase (33). Another point noticed is that H3K27me3 is mainly responsible for silencing genes, so it usually acts as a transcriptional suppressor (34). It has been reported that EZH2 played a significant role in multiple tumor progression by affecting cellular senescence (35, 36). In particular matter-induced skin keratinocytes senescence, skin senescence depends on AhR-induced ROS and the decrease in EZH2 and H3K27me3(37). Meanwhile, AhR activation could enhance EZH2 activity and increase its epigenetic silencing activity, which is a risk factor for environmental toxicant-associated pancreatitis and pancreatic cancer (28). Not only that, EZH2 binds to the AhR promoter to repress the expression of AhR gene (38). From this, we thought EZH2 might play a key role in AhR-induced cellular senescence. Herein, we firstly investigated the correlation between AhR and EZH2. As expected, our results revealed that the mRNA levels of AhR and EZH2 were significantly correlated in the RNA-sequencing data of cisplatin-stimulated mice. Cisplatin stimulation concurrently up-regulated AhR and EZH2 expression, and AhR inhibitor BAY2416964 or tubule specific AhR deficiency suppressed the expression of EZH2. *In vitro*, the expression of AhR and EZH2 were increased in cisplatin-treated TCMK-1 cells. The AhR knockdown reversed the elevation of AhR as well as EZH2, which was consistent with the results *in vivo*, suggesting that EZH2 may be a possible mediator in AhR-induced cellular senescence. Importantly, considering the crucial role of EZH2 in epigenetic regulation and combining with the previous research results of Ko et al.(38), we further explored the influence of EZH2 knockdown on the expression of AhR in cisplatin-induced TCMK-1 cells. Surprisingly, EZH2 silencing in cisplatin-treated TCMK-1 cells reversely repressed the upregulation of AhR. To illustrate how EZH2 regulates AhR, we used a ChIP assay to examine the enrichment between EZH2 or H3K27me3 and the AhR promoter regions. Consequently, H3K27me3 is responsible for exerting transcriptional inhibition effect in the control mice, because of the rich enrichment between H3K27me3 and AhR promoter region, which repressed the expression of AhR. Nevertheless, the weaken enrichment of them has been described in the cisplatin mice, indicating that the rare enrichment of H3K27me3 and AhR promoter might cause cisplatin-induced AhR expression. These

findings, therefore, identify that EZH2 also is one of the positive regulators of AhR expression by affecting the enrichment between H3K27me3 and AhR promoter.

In conclusion, our finding demonstrated that AhR was highly expressed in cisplatin-induced kidney tissues. AhR inhibition repressed cisplatin-induced cellular senescence and attenuated kidney injury. Furthermore, AhR could serve as an upstream regulator to upregulate the expression of EZH2, which mediated cisplatin-induced cellular senescence. Notably, EZH2 could reversely exert epigenetic regulation to form a positive feedback loop with AhR. Nevertheless, the detailed regulatory network involving AhR-EZH2-cellular senescence is remarkably lacking. Collectively, the present study confers new data on the mechanism by which AhR upregulates EZH2 to accelerate tubular cell senescence in cisplatin-induced AKI.

Material And Methods

Agent, antagonist and antibodies

Cisplatin and BAY 2416964 were purchased from Synguider (Chengdu, China) and Selleck Chemicals (America), respectively. All primary antibodies were displayed in Supplementary Table 1.

Animal experiments

Animal experimental procedures were licensed and permitted by the Animal Care and Use Ethics Committee of Sichuan University (2020205A). Male C57BL/6J mice were clarified previously(27). C57BL/6J mice were administered cisplatin (20 mg/kg) with or without BAY 2416964 (20 mg/kg) by intraperitoneal injection. Tubule specific AhR knockout mice were obtained from the GemPharmatech Co.,Ltd. (Jiangsu, China). AhR tecKO mice were injected cisplatin intraperitoneally to induce AKI.

Cell culture and treatment

Mouse renal tubular epithelial cells (TCMK-1) were cultured in MEM medium (G4550-500ML, Sercicebio) containing 10% fetal bovine serum (FBS) (SH30084.03, Hyclone) at 37 °C under 5% CO2-95% air environment. TCMK-1 cells were starved in 0.5% FBS medium for 6h and then treated with 10μg/ml cisplatin for another 24h. The siRNAs were used to knock down AhR and EZH2. The transfection procedure is detailed in the riboFECT ^{TM} CP transfection kit instruction. AhR-siRNA, EZH2-siRNA and negative control (NC) siRNA were designed and synthesized by GenePharma

(Shanghai, China). The detailed transfection sequences information of them is provided in Supplementary Table 2.

Single-cell data analysis

The single-cell RNA sequencing database from http://humphreyslab.com/SingleCell/ was used for single-cell data analysis. According to the database, we checked the single-cell RNA sequencing data about AhR

in the healthy adult humans, healthy mice, and ischemia-reperfusion injury (IR/I) mouse kidneys.

Renal function assay

An automatic biochemical analyzer (Mindray BS-240) was taken to assess Scr and BUN. We defined that the cisplatin-induced AKI mouse model was successfully established, when the Scr value in the cisplatin group was higher than twice that in the control group.

Pathological examination

The kidney tissues were fixed, embedded, and sectioned for Periodic Acid-Schiff (PAS) staining. Renal tubular damage semi-quantitatively scores were used to assess the pathological injury. The specific score standards and detailed rules have been shown in previous study(27).

Immunofluorescence staining

Paraffin kidney tissue sections were firstly deparaffinized and dehydrated. Then, using the microwave method repairs the antigen. After antigen retrieval, the sections were sealed with 1× horse serum containing 0.3% Triton (Sigma, America) for 1h at 37℃. And then, they were incubated with primary antibody (the concentration is determined according to the instructions) overnight at 4°C. Washing the sections and incubating the corresponding secondary antibody and lectin (1:400 dilution) for 1h at room temperature. Then, the sections were rewashed. DAPI (D8200; Solarbio) was used to stain nuclei for 5min. Finally,50% glycerin was used to seal the sections. Photographs were collected from ZEN 2012 microscopy software.

Senescence β-galactosidase staining

The senescence β-galactosidase staining kit (Cell Signaling Technology) was used to detect β-galactosidase activity, a known characteristic of senescent cells. For SA β-Gal staining of frozen renal tissues, frozen sections were fixed with 1× fixative solution for 10-15min at room temperature. Washing the sections with 1× PBS. Then, added the β-galactosidase staining solution to the sections and incubated them at 37°C overnight in a dry incubator (no CO2). The senescent cells showed blue color under a microscope.

ChIP assay

Proteins and DNA interaction was evaluated by ChIP-qPCR using the ChIP assay kit (Millipore, MA, USA). The experiment protocols were according to the manufacturer's instructions. The antibodies used for the ChIP assay were as follows: anti-H3k27me3 (Cell Signaling Technology) and control IgG (Millipore). The primers used for ChIP were as follows: AhR-F 5'-GTCAACGACATTTGCGTCCT-3', AhR-R 5'-TCCCCTTAAGAATTTCAACTGTCC-3'. The calculation formula for enrichment efficiency was elaborated on previously(27).

Western blot analysis

Western blotting was carried out as described earlier(27). Densitometry analysis was evaluated by using ImageJ 6.0 software (National Institutes of Health, Bethesda, MD, USA). Gray density was normalized using internal reference proteins GAPDH or Histone 3. To ensure the repeatability of the experiment, all immunoblot bands were repeated three times.

Quantitative real-time reverse transcriptase PCR (RT-qPCR)

Total RNA separation and purification steps and RT-qPCR protocols were displayed as previously shown(27). The corresponding gene primers were listed in Table S2. The $2^{-\Delta\Delta Ct}$ method was used to calculate the relative gene quantities, and GAPDH was used as the internal reference gene.

Statistical analysis

All quantitative data were presented as mean ± standard deviation (SD). Statistical difference comparisons between the two groups were performed using the T-test. Comparisons between three or multiple groups were performed using a one-way analysis of variance (Tukey's test). Prism 9.0 (GraphPad Software, San Diego, CA, USA) was used to draw statistical graphs, and P value less than 0.05 was considered statistically significant.

Declarations

Acknowledgements

This study was supported by a grant from the National Key R&D Program of China (No. 2020YFC2005000), the National Natural Science Foundation of China (82070711) and the Science/Technology Project of Sichuan province (No. 2020YFQ0055).

Author Contribution Statement

L.M., and L.W. designed experiments. L.W., Q.R., F.G., Y.L., and L.M. performed experiments. L.W. and L.M. analyzed the data. L.W., and L.M., wrote the draft of the manuscript. All author approved the submission.

Conflict of Interest Statement

The authors declare no competing interests.

References

1. Wen X, Murugan R, Peng Z, Kellum JA. Pathophysiology of Acute Kidney Injury: A New Perspective. Contributions to Nephrology. 2010;165:39-45.
2. Lameire NH, Bagga A, Cruz D, De Maeseneer J, Endre Z, Kellum JA, et al. Acute kidney injury: an increasing global concern. The Lancet. 2013;382(9887):170-9.
3. Ronco C, Bellomo R, Kellum JA. Acute kidney injury. The Lancet. 2019;394(10212):1949-64.

4. Bawaskar PH, Bawaskar PH, Bawaskar HS. Eliminating acute kidney injury by 2025: an achievable goal for India. The Lancet. 2015;386(9996):855.
5. Fu Y, Tang C, Cai J, Chen G, Zhang D, Dong Z. Rodent models of AKI-CKD transition. American Journal of Physiology-Renal Physiology. 2018;315(4):F1098-F106.
6. Coelho S, Cabral G, Lopes JA, Jacinto A. Renal regeneration after acute kidney injury. Nephrology. 2018;23(9):805-14.
7. Guo C, Dong G, Liang X, Dong Z. Epigenetic regulation in AKI and kidney repair: mechanisms and therapeutic implications. Nature Reviews Nephrology. 2019;15(4):220-39.
8. Naughton CA. Drug-induced nephrotoxicity. Am Fam Physician. 2008;78(6):743-50.
9. Li C, Xie N, Li Y, Liu C, Hou FF, Wang J. N-acetylcysteine ameliorates cisplatin-induced renal senescence and renal interstitial fibrosis through sirtuin1 activation and p53 deacetylation. Free Radical Biology and Medicine. 2019;130:512-27.
10. Sears SM, Siskind LJ. Potential Therapeutic Targets for Cisplatin-Induced Kidney Injury: Lessons from Other Models of AKI and Fibrosis. Journal of the American Society of Nephrology. 2021;32(7):1559.
11. Andrade L, Rodrigues CE, Gomes SA, Noronha IL. Acute Kidney Injury as a Condition of Renal Senescence. Cell Transplantation. 2018;27(5):739-53.
12. Johnson AC, Zager RA. Plasma and urinary p21: potential biomarkers of AKI and renal aging. American Journal of Physiology-Renal Physiology. 2018;315(5):F1329-F35.
13. Morigi M, Perico L, Rota C, Longaretti L, Conti S, Rottoli D, et al. Sirtuin 3–dependent mitochondrial dynamic improvements protect against acute kidney injury. The Journal of clinical investigation. 2015;125(2):715-26.
14. Wang W-g, Sun W-x, Gao B-s, Lian X, Zhou H-l. Cell Cycle Arrest as a Therapeutic Target of Acute Kidney Injury. Current Protein & Peptide Science. 2017;18(12):1224-31.
15. Vondráček J, Machala M. Environmental Ligands of the Aryl Hydrocarbon Receptor and Their Effects in Models of Adult Liver Progenitor Cells. Stem Cells International. 2016;2016:4326194.
16. Hankinson O. The aryl hydrocarbon receptor complex. Annu Rev Pharmacol Toxicol. 1995;35:307-40.
17. Tao S, Guo F, Ren Q, Liu J, Wei T, Li L, et al. Activation of aryl hydrocarbon receptor by 6-formylindolo[3,2-b]carbazole alleviated acute kidney injury by repressing inflammation and apoptosis. Journal of Cellular and Molecular Medicine. 2021;25(2):1035-47.
18. Eleftheriadis T, Pissas G, Filippidis G, Liakopoulos V, Stefanidis I. The Role of Indoleamine 2,3-Dioxygenase in Renal Tubular Epithelial Cells Senescence under Anoxia or Reoxygenation. Biomolecules. 2021;11(10).
19. Wu H, Malone AF, Donnelly EL, Kirita Y, Uchimura K, Ramakrishnan SM, et al. Single-Cell Transcriptomics of a Human Kidney Allograft Biopsy Specimen Defines a Diverse Inflammatory Response. (1533-3450 (Electronic)).

20. Wu H, Kirita Y, Donnelly EL, Humphreys BD. Advantages of Single-Nucleus over Single-Cell RNA Sequencing of Adult Kidney: Rare Cell Types and Novel Cell States Revealed in Fibrosis. (1533-3450 (Electronic)).
21. Kirita Y, Wu H, Uchimura K, Wilson Parker C, Humphreys Benjamin D. Cell profiling of mouse acute kidney injury reveals conserved cellular responses to injury. Proceedings of the National Academy of Sciences. 2020;117(27):15874-83.
22. Späth MR, Bartram MP, Palacio-Escat N, Hoyer KJR, Debes C, Demir F, et al. The proteome microenvironment determines the protective effect of preconditioning in cisplatin-induced acute kidney injury. Kidney international. 2019;95(2):333-49.
23. Ferenbach DA, Bonventre JV. Mechanisms of maladaptive repair after AKI leading to accelerated kidney ageing and CKD. (1759-507X (Electronic)).
24. Ren F, Ji C, Huang Y, Aniagu S, Jiang Y, Chen T. AHR-mediated ROS production contributes to the cardiac developmental toxicity of PM2.5 in zebrafish embryos. Science of The Total Environment. 2020;719:135097.
25. Yang H, Fogo AB. Cell Senescence in the Aging Kidney. Journal of the American Society of Nephrology. 2010;21(9):1436.
26. Yabuuchi N, Hou H, Gunda N, Narita Y, Jono H, Saito H. Suppressed Hepatic Production of Indoxyl Sulfate Attenuates Cisplatin-Induced Acute Kidney Injury in Sulfotransferase 1a1-Deficient Mice. International journal of molecular sciences. 2021;22(4).
27. Wen L, Tao S-h, Guo F, Li L-z, Yang H-l, Liang Y, et al. Selective EZH2 inhibitor zld1039 alleviates inflammation in cisplatin-induced acute kidney injury partially by enhancing RKIP and suppressing NF-κB p65 pathway. Acta Pharmacologica Sinica. 2021.
28. Lee J-e, Cho S-G, Ko S-G, Ahrmad SA, Puga A, Kim K. Regulation of a long noncoding RNA MALAT1 by aryl hydrocarbon receptor in pancreatic cancer cells and tissues. Biochemical and biophysical research communications. 2020;532(4):563-9.
29. Sharp CN, Doll MA, Dupre TV, Shah PP, Subathra M, Siow D, et al. Repeated administration of low-dose cisplatin in mice induces fibrosis. American Journal of Physiology-Renal Physiology. 2016;310(6):F560-F8.
30. Walker JA, Richards S, Belghasem ME, Arinze N, Yoo SB, Tashjian JY, et al. Temporal and tissue-specific activation of aryl hydrocarbon receptor in discrete mouse models of kidney disease. Kidney international. 2020;97(3):538-50.
31. Dou L, Poitevin S, Sallée M, Addi T, Gondouin B, McKay N, et al. Aryl hydrocarbon receptor is activated in patients and mice with chronic kidney disease. Kidney international. 2018;93(4):986-99.
32. Ren Q, Cheng L, Guo F, Tao S, Zhang C, Ma L, et al. Fisetin Improves Hyperuricemia-Induced Chronic Kidney Disease via Regulating Gut Microbiota-Mediated Tryptophan Metabolism and Aryl Hydrocarbon Receptor Activation. Journal of Agricultural and Food Chemistry. 2021;69(37):10932-42.

33. Schuettengruber B, Chourrout D, Vervoort M, Leblanc B, Cavalli G. Genome Regulation by Polycomb and Trithorax Proteins. Cell. 2007;128(4):735-45.
34. Sauvageau M, Sauvageau G. Polycomb group proteins: multi-faceted regulators of somatic stem cells and cancer. Cell Stem Cell. 2010;7(3):299-313.
35. Liu C, Liu L, Yang M, Li B, Yi J, Ai X, et al. A positive feedback loop between EZH2 and NOX4 regulates nucleus pulposus cell senescence in age-related intervertebral disc degeneration. Cell Division. 2020;15(1):2.
36. Chen Y, Pan K, Wang P, Cao Z, Wang W, Wang S, et al. HBP1-mediated Regulation of p21 Protein through the Mdm2/p53 and TCF4/EZH2 Pathways and Its Impact on Cell Senescence and Tumorigenesis*. Journal of Biological Chemistry. 2016;291(24):12688-705.
37. Ryu YS, Kang KA, Piao MJ, Ahn MJ, Yi JM, Bossis G, et al. Particulate matter-induced senescence of skin keratinocytes involves oxidative stress-dependent epigenetic modifications. Experimental & molecular medicine. 2019;51(9):1-14.
38. Ko C-I, Wang Q, Fan Y, Xia Y, Puga A. Pluripotency factors and Polycomb Group proteins repress aryl hydrocarbon receptor expression in murine embryonic stem cells. Stem Cell Res. 2014;12(1):296-308.

Figures

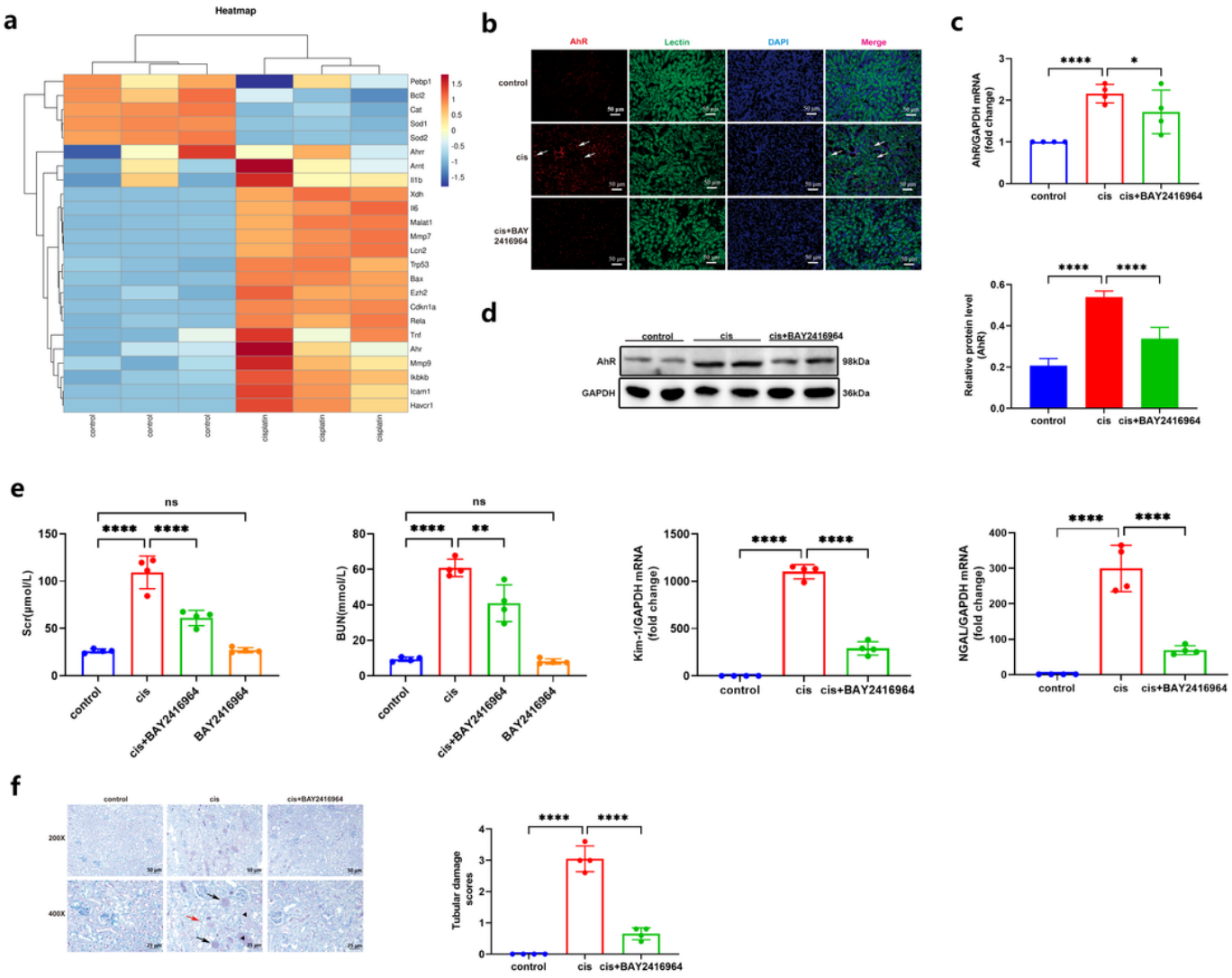

Figure 1

AhR antagonist BAY2416964 alleviates kidney injury in cisplatin-induced mice. (a) The cluster heatmap was conducted to present differentially expressed genes in the GSE106993 dataset (n=3). **(b)** Representative micrographs (×200) illustrated AhR (red) immunofluorescence staining of kidney tissues. **(c, d)** The mRNA and protein levels of AhR, and the relative protein level of AhR was quantified by densitometry and normalized with GAPDH (n=3); All western blot protein samples were taken from two random mice in different group, and the experiments were repeated three times. **(e)** The biochemical levels and mRNA expression of Kim-1 and NGAL (n=4); **(f)** Representative PAS staining sections of kidney tissues were magnified ×200 and ×400, and tubular damage scores were calculated. Data are represented as means ± SDs (n=4). $^{****}P < 0.0001$, $^{**}P < 0.01$, $^{*}P < 0.05$, $^{ns}P > 0.05$.

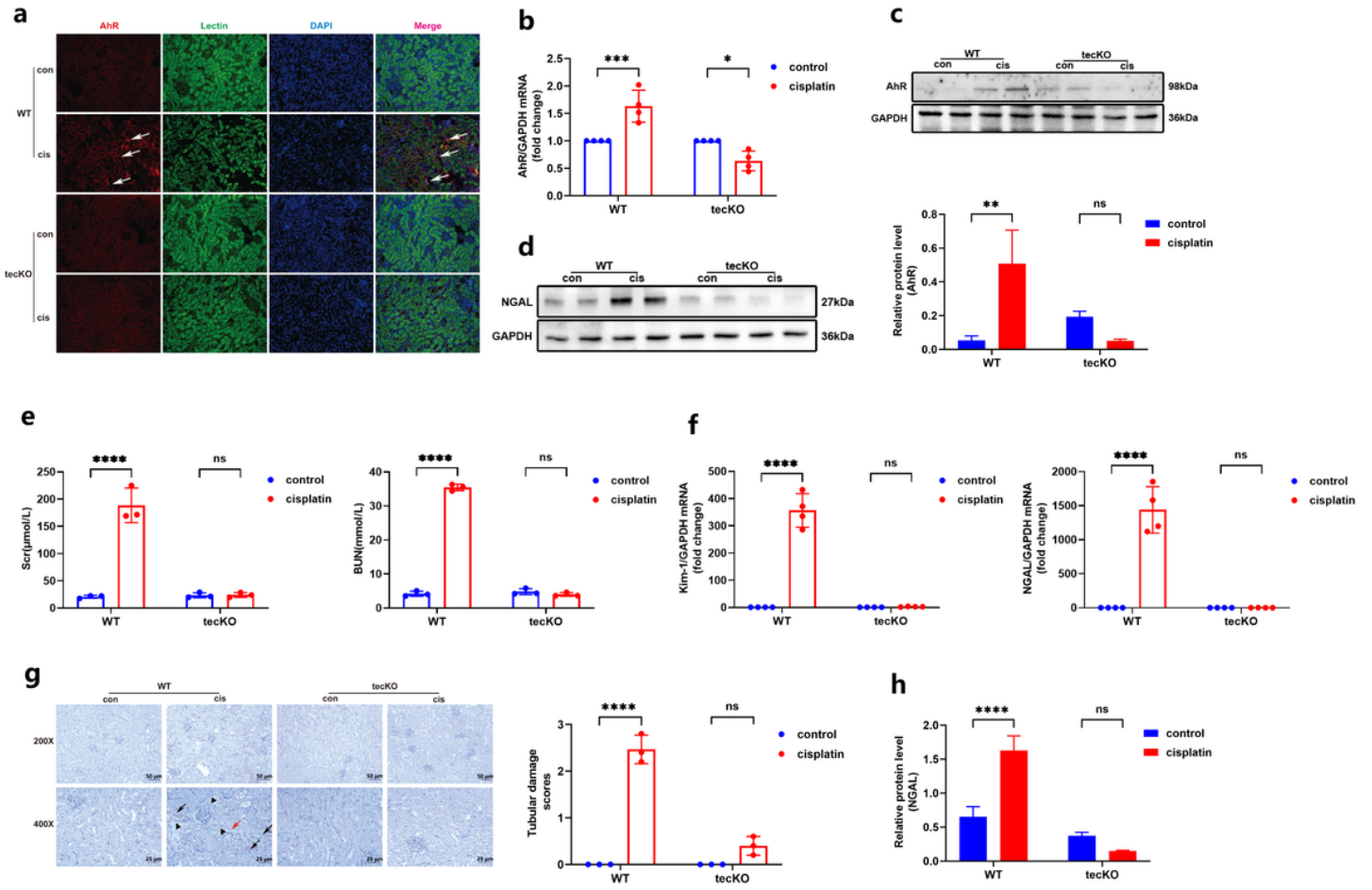

Figure 2

Renal tubular epithelial cell-specific AhR deletion improves cisplatin-induced kidney injury in mice. (a) Representative micrographs (×200) illustrated AhR (red) immunofluorescence staining of kidney tissues in cisplatin-induced WT or AhR tecKO mice. **(b)** The AhR mRNA level by RT-qPCR (n=4). **(c)** The AhR protein level by western blot and the relative protein level was quantified by densitometry and normalized with GAPDH (n=3). **(d, h)** NGAL expression and the relative protein level was quantified by densitometry and normalized with GAPDH (n=3); All western blot analysis was performed in two randomized mice from each group, and the experiments were repeated in triplicate. **(e)** Scr and BUN levels in cisplatin-induced WT or AhR tecKO mice. **(f)** The Kim-1, NGAL mRNA levels by RT-qPCR (n=4); **(g)** Representative PAS staining sections (×200 and ×400) and tubular damage scores (n = 3). Data are represented as means ± SDs. $^{****}P < 0.0001$, $^{**}P < 0.01$, $^{*}P < 0.05$, $^{ns}P > 0.05$.

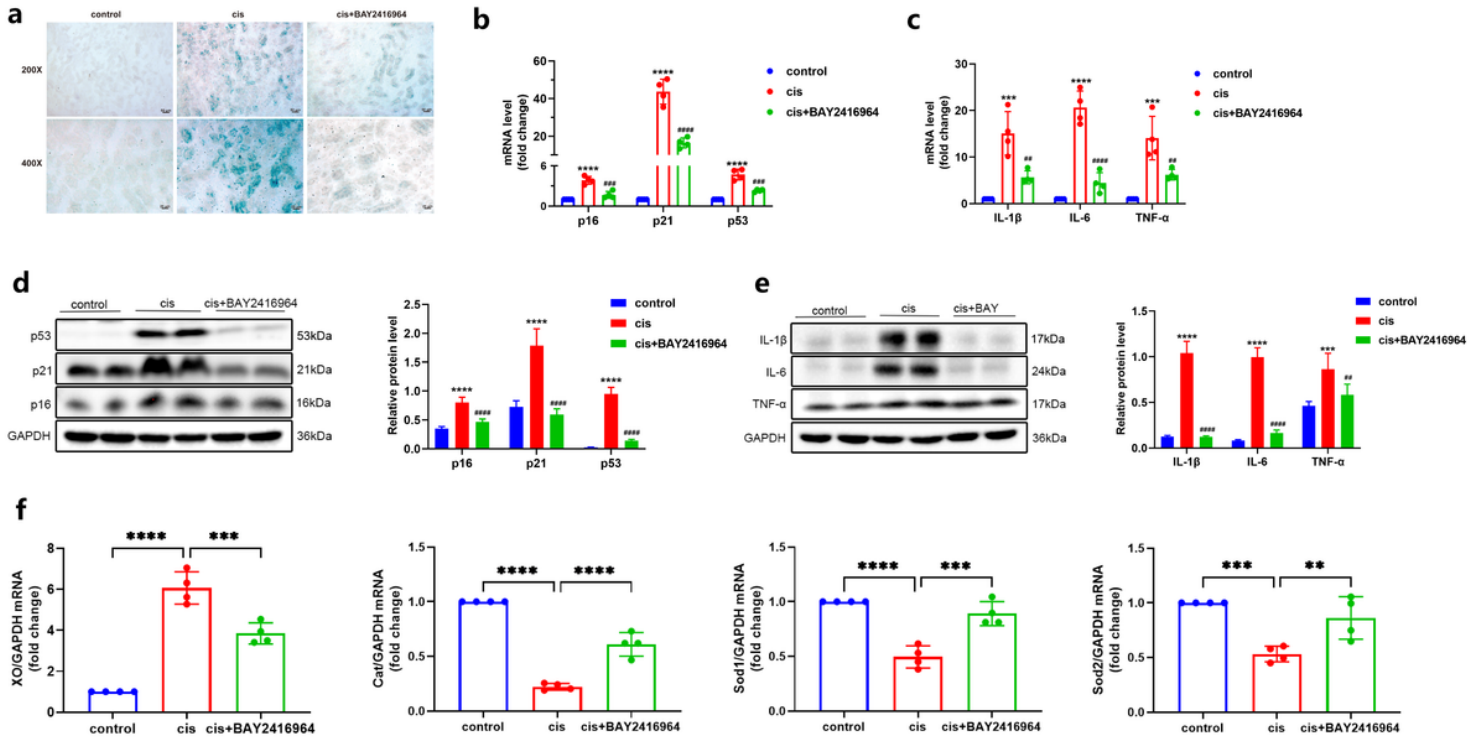

Figure 3

AhR inhibition by BAY2416964 was accompanied by suppressed tubular cellular senescence and oxidative stress in cisplatin-induced AKI mice. (a) Representative cellular senescence photographs of SA-β-Gal staining in cisplatin-induced kidneys (magnification ×200 and ×400); Blue: SA β-gal positive region. **(b)** The mRNA levels of p16, p21 and p53 in different groups of mice (n=4). **(c)** The mRNA levels of IL-1β, IL-6 and TNFα (n=4). **(d)** Protein expression of p16, p21 and p53 were quantified by densitometry and normalized with GAPDH; **(e)** Protein expression of IL-1β, IL-6 and TNFα were quantified by densitometry and normalized with GAPDH; $^{****}P < 0.0001$, $^{***}P < 0.001$ compared with the control group; $^{####}P < 0.0001$, $^{###}P < 0.001$, $^{##}P < 0.01$ compared with the cisplatin group. All western blot analysis was performed in two randomized mice from each group, and the experiments were repeated in triplicate. **(f)** The mRNA expression of XO, Cat, Sod1 and Sod2 (n=4); Data are represented as means ± SDs, $^{****}P < 0.0001$, $^{***}P < 0.001$, $^{**}p < 0.01$.

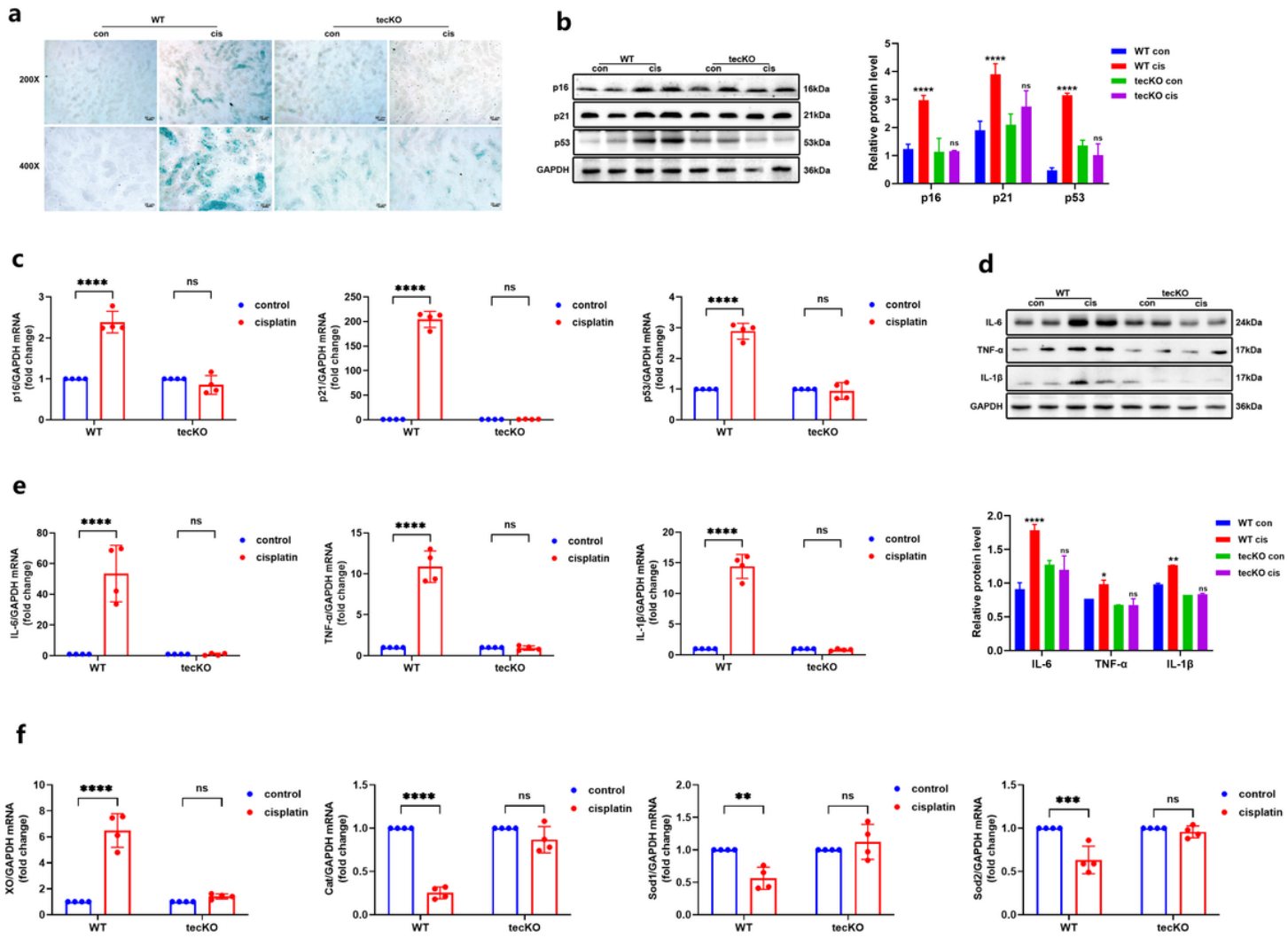

Figure 4

AhR deficiency improved cellular senescence and reduced oxidative stress in cisplatin-induced AKI mice. **(a)** Representative images of SA β-Gal staining in cisplatin-induced WT and AhR tecKO mice (magnification ×200 and ×400). Blue: SA β-Gal positive region. **(b)** Protein expression of SAGs (p16, p21, p53) and **(d)** SASPs (IL-1β, IL-6, TNF-α) shown by western blot in WT and AhR tecKO mice with or without cisplatin administration, and the relative protein level was quantified by densitometry and normalized with GAPDH (n=3); $^{****}P < 0.0001$, $^{**}P < 0.01$, $^{*}P < 0.05$ compared with WT control group; $^{ns}P > 0.05$ compared with tecKO control group. All western blot protein samples were taken from two random mice in different group, and the experiments were repeated three times. **(c)** Transcript expression of SAGs (p16, p21, p53) and **(e)** SASPs (IL-1β, IL-6, TNF-α) in WT and AhR tecKO mice with or without cisplatin administration (n=4). **(f)** Oxidant (XO) and anti-oxidant (Cat, Sod1, Sod2) expression, measured by RT-qPCR in WT and AhR tecKO mice with or without cisplatin administration (n=4). Data are represented as means ± SDs, $^{****}P < 0.0001$, $^{***}P < 0.001$, $^{**}p < 0.01$, $^{ns}P > 0.05$.

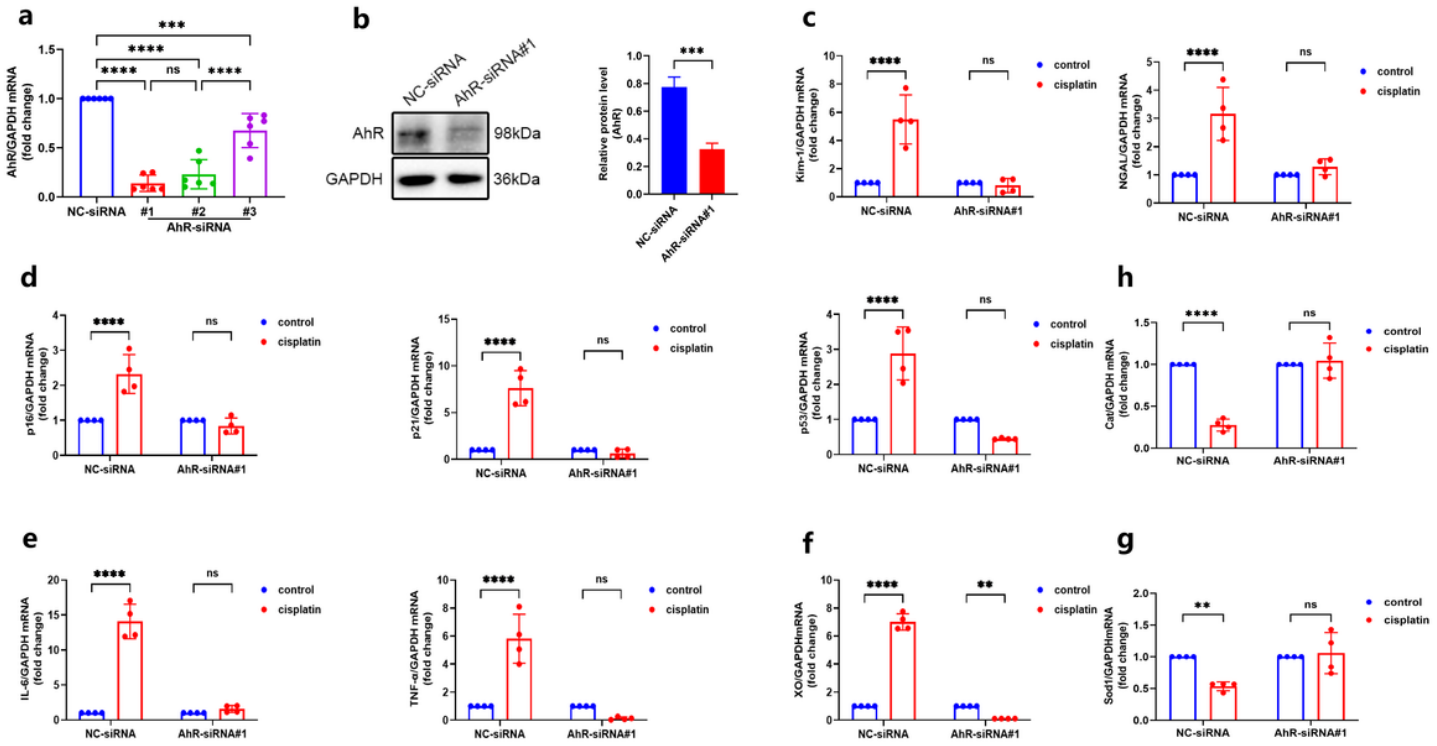

Figure 5

AhR knockdown attenuates cellular injury and senescence as well as represses oxidative stress in cisplatin-stimulated TCMK-1 cells. (a) Screening for suitable AhR-siRNA. **(b)** AhR protein level in TCMK-1 cells, and the relative protein level was quantified by densitometry and normalized with GAPDH (n=3). All western blot experiments were repeated in triplicate. **(c)** Transcript expression of Kim-1 and NGAL in TCMK-1 cells with or without cisplatin stimulation (n=4). **(d)** Transcript expression of SAGs (p16, p21, p53) and **(e)** SASPs (IL-1β, IL-6, TNF-α) in TCMK-1 cells with or without cisplatin stimulation (n=4). **(f)** Oxidant (XO) and **(g, h)** anti-oxidant (Cat, Sod1) expression, measured by RT-qPCR in TCMK-1 cells with or without cisplatin stimulation (n=4). Data are represented as means ± SDs, $^{****}P < 0.0001$, $^{***}P < 0.001$, $^{**}p < 0.01$, $^{ns}P > 0.05$.

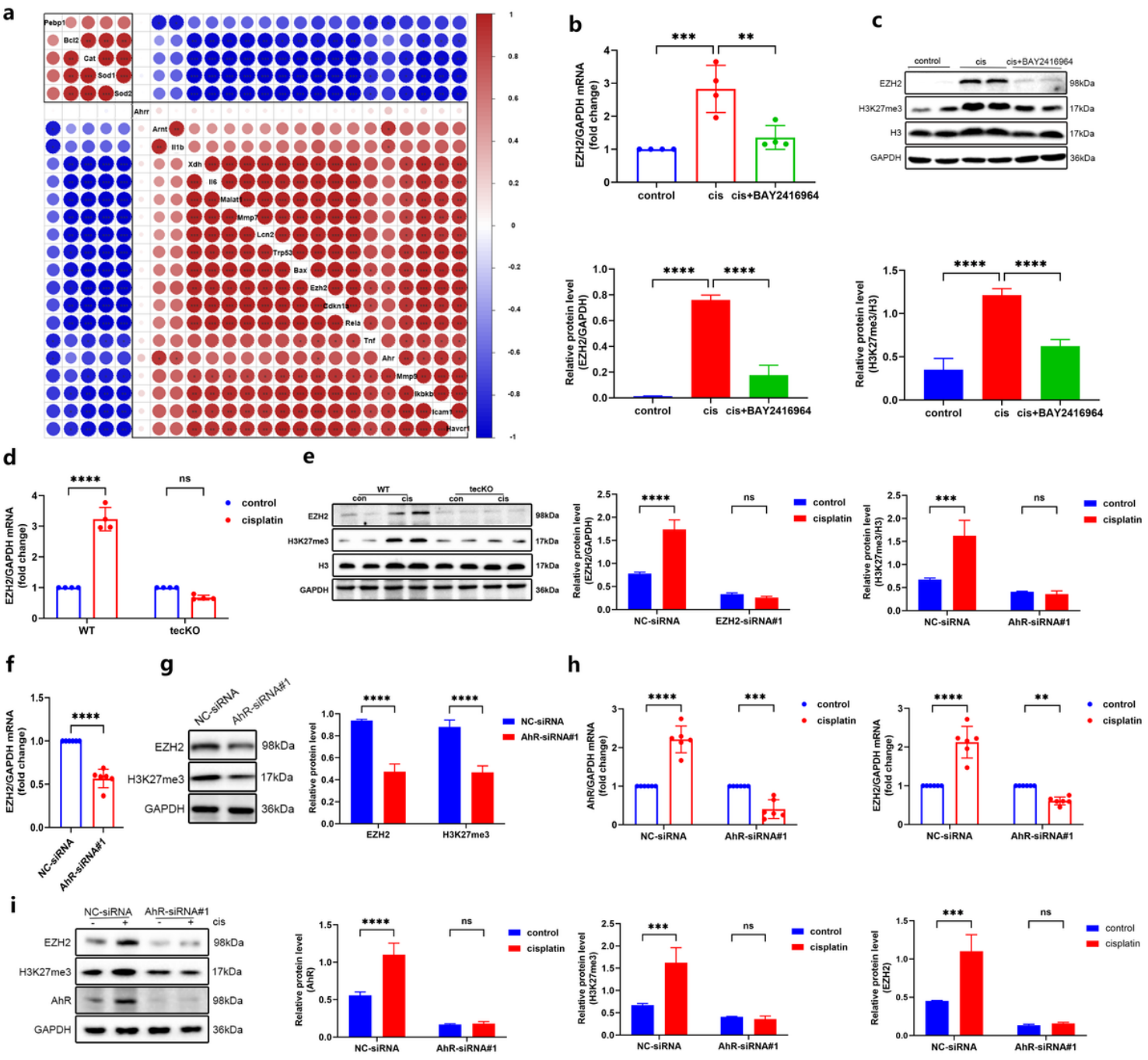

Figure 6

AhR triggers EZH2 and H3K27me3 expression after cisplatin stimulation. (a) Correlation in differentially expressed genes were displayed by the correlation heatmap. **(b)** The mRNA level of EZH2 in different groups of mice (n=4). **(c)** Protein expression of EZH2 and H3K27me3 were shown, and gray densitometry were quantified and normalized with GAPDH (n=3); **(d)** The mRNA level of EZH2 in WT and AhR tecKO mice with or without cisplatin administration (n=4). **(e)** Protein expression of EZH2 and H3K27me3 were shown in WT and AhR tecKO mice with or without cisplatin administration, and the relative protein level was quantified by densitometry and normalized with GAPDH or H3 (n=3). **(f)** Transcript expression (n=6) and **(g)** protein level (n=3) of EZH2 in TCMK-1 cells. **(h)** Transcript expression (n=6) and **(i)** protein level

(n=3) of AhR and EZH2 in NC-siRNA and AhR-siRNA#1 TCMK-1 cells with or without cisplatin stimulation. All western blot experiments were repeated in triplicate. Data are represented as means ± SDs, $^{****}P < 0.0001$, $^{***}P < 0.001$, $^{**}p < 0.01$, $^{ns}P > 0.05$.

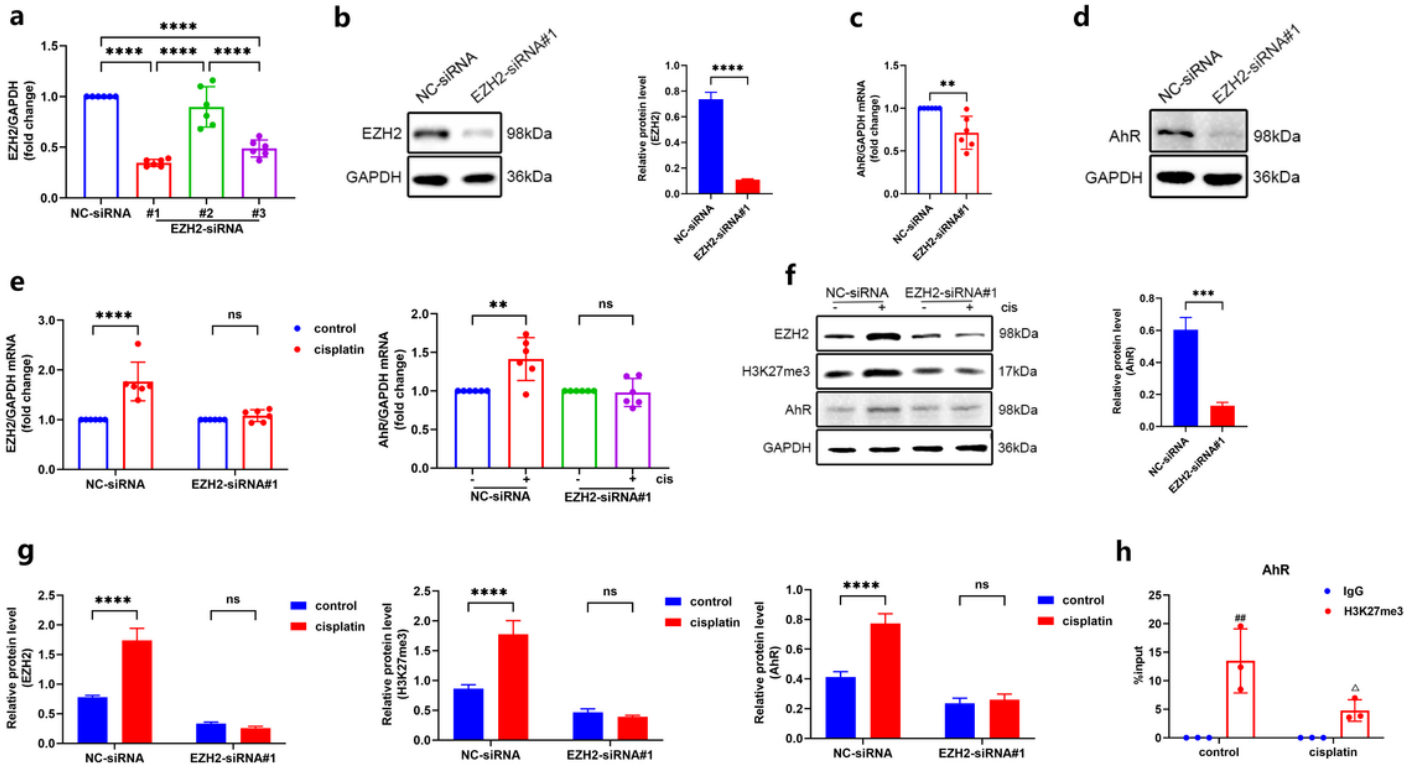

Figure 7

EZH2 reversely regulates AhR expression in TCMK-1 cells. (a) Screening for suitable EZH2-siRNA through mRNA expression level. **(b)** EZH2 protein level in NC-siRNA and EZH2-siRNA#1 TCMK-1 cells, and the relative protein level was quantified by densitometry and normalized with GAPDH (n=3). **(c)** Transcript expression (n=6) and **(d)** protein level (n=3) of AhR in NC-siRNA and EZH2-siRNA#1 TCMK-1 cells. **(e)** Transcript expression (n=6) and **(f)** protein level (n=3) of EZH2 and AhR in NC-siRNA and EZH2-siRNA#1 TCMK-1 cells with or without cisplatin stimulation, **(g)** the relative protein levels of them were quantified by densitometry and normalized with GAPDH (n=3), all western blot experiments were repeated in triplicate, $^{****}P < 0.0001$, $^{***}P < 0.001$, $^{**}p < 0.01$, $^{ns}P > 0.05$. **(h)** Control and cisplatin mice kidney tissues were performed to ChIP-qPCR assay using immunoglobulin G (IgG) and the H3K27me3 antibody (n = 3). Data are represented as means ± SDs, $^{\#\#}P < 0.01$ compared with the control group IgG antibody. $^{\triangle}P < 0.05$ compared with the cisplatin group H3K27me3 antibody.

Supplementary Files

This is a list of supplementary files associated with this preprint. Click to download.

- RawWesternBlotImages.docx

- Supplementarymaterial.docx